ARTICLE
Journal of Cellular Biochemistry 116:1361–1370 (2015)

Journal of Cellular Biochemistry

Hirsutenone Directly Targets PI3K and ERK to Inhibit Adipogenesis in 3T3-L1 Preadipocytes

Lai Yee Cheong,[1] Sujin Suk,[2] N. R. Thimmegowda,[3] Min-Yu Chung,[1,4] Hee Yang,[1] Sang Gwon Seo,[1] B. Shwetha,[3] Jong-Eun Kim,[1,5] Jung Yeon Kwon,[6] Bo Yeon Kim,[3] and Ki Won Lee[1,2,5,6]*

[1]*WCU Biomodulation Major, Department of Agricultural Biotechnology and Center for Food and Bioconvergence, Seoul National University, Seoul, Republic of Korea*

[2]*Interdisciplinary Program in Agricultural Biotechnology Major, College of Agriculture and Life Sciences, Seoul National University, Seoul, Republic of Korea*

[3]*Chemical Biology Research Center and World Class Institute, Korea Research Institute of Bioscience and Biotechnology, Ochang, Republic of Korea*

[4]*Division of Metabolism and Functionality Research, Korea Food Research Institute, Seongnam, Republic of Korea*

[5]*Research Institute of Bio Food Industry, Institute of Green Bio Science and Technology, Seoul National University, Pyeongchang, Republic of Korea*

[6]*Advanced Institutes of Convergence Technology, Seoul National University, Suwon, Republic of Korea*

ABSTRACT

Adipogenesis is a key driver of the expansion of adipose tissue mass that causes obesity. Hirsutenone (HST) is an active botanical diarylheptanoid present in *Alnus* species. In this study, we evaluated the effects of HST on adipogenesis, its mechanisms of action and the molecular targets involved. Using Oil Red O staining, we observed that HST dose-dependently suppresses lipid accumulation during adipogenesis in 3T3-L1 preadipocytes, concomitant with a decrease in peroxisome proliferator-activated receptor-γ (PPARγ), CCAAT/enhancer-binding protein α (C/EBPα) and fatty acid synthase (FAS) protein expression. This inhibitory effect was largely limited to the early stage of adipogenesis, which includes mitotic clonal expansion (MCE), as evidenced by delayed cell cycle entry of preadipocytes from G1 to S phase. Furthermore, the regulation of MCE was accompanied by suppression of phosphatidylinositol 3-kinase (PI3K) and extracellular-regulated kinase (ERK) activity. HST was also shown to bind directly to PI3K and ERK1 in a non-ATP competitive manner. Our results suggest that HST attenuates adipogenesis by directly targeting PI3K and ERK during MCE in 3T3-L1 preadipocytes, underscoring the potential therapeutic application of HST in preventing obesity. J. Cell. Biochem. 116: 1361–1370, 2015.

KEY WORDS: ADIPOGENESIS; HIRSUTENONE; MITOTIC CLONAL EXPANSION; ERK; PI3K

Obesity has become a global epidemic and is the fifth leading cause of deaths worldwide. More than 1.4 billion adults aged 20 and older are currently overweight and at least 500 million are classified as obese as reported by World Health Organization in 2014. Obesity develops when energy intake chronically exceeds energy expenditure. Excess energy is then stored as triglycerides in adipocytes, promoting the expansion of adipose mass through hypertrophy (increased cell size) and hyperplasia (increased cell

Abbreviations used: C/EBPα, CCAT/enhancer-binding protein-α; ERK, extracellular-related kinase; FAS, fatty acid synthase; HST, hirsutenone; MCE, mitotic clonal expansion; PI3K, phosphatidylinositol 3-kinase; PPARγ, peroxisome proliferator-activated receptor-γ.

Conflict of interest: None of the authors declare any conflict of interest.

Lai Yee Cheong, Sujin Suk, and N.R. Thimmegowda equally contributed to the work.

Grant sponsor: Leap Research Program; Grant number: 2010-0029233; Grant sponsor: National Research Foundation; Grant number: 2012M3A9C4048818; Grant sponsor: Ministry of Science, ICT and Future Planning.

* Correspondence to: Ki Won Lee, Department of Agricultural Biotechnology, Seoul National University, Seoul, Republic of Korea. E-mail: kiwon@snu.ac.kr

Manuscript Received: 18 September 2014; Manuscript Accepted: 23 January 2015

Accepted manuscript online in Wiley Online Library (wileyonlinelibrary.com): 10 March 2015

DOI 10.1002/jcb.25093 • © 2015 Wiley Periodicals, Inc.

number) as adipose tissue remodels and adapts to the nutritional environment in the body [Anthony et al., 2009; Mishra et al., 2013]. However, the processes of adipocyte hypertrophy and hyperplasia are frequently accompanied with intracellular abnormalities in adipocyte function, which contribute to the development of metabolic diseases including type 2 diabetes [de Ferranti and Mozaffarian, 2008].

Adipogenesis is a process of cell differentiation from preadipocytes to mature adipocytes, and can be divided into three phases: the early phase, including mitotic clonal expansion (MCE), the intermediate phase, and late phase of differentiation [Witczak et al., 2008; Cristancho and Lazar, 2011; Lai et al., 2012]. In particular, MCE is a prerequisite stage for terminal differentiation where growth-arrested cells synchronously re-enter the cell cycle, leading to an increase in cell numbers [Tang et al., 2003a,b; Zhang et al., 2004]. Considering its role in adipose tissue expansion, the control of adipogenesis has been proposed as a critical approach for preventing obesity [Sun et al., 2013].

3T3-L1 preadipocytes are one of the most widely used models for studying aspects of adipocyte biology, including adipogenesis. In order to induce adipogenic differentiation of 3T3-L1 preadipocytes, the addition of glucocorticoids, cAMP enhancer and insulin is required. This initiates a transcriptional regulatory cascade that results in a gene expression profile specific for adipocyte function, involving the expression of CCAT/enhancer-binding proteins (C/EBPs), peroxisome proliferator-activated receptor-γ (PPARγ) and fatty acid synthase (FAS) [Rosen et al., 2000]. In particular, insulin has a remarkable influence on adipogenesis in vitro and in vivo by promoting preadipocyte differentiation and enhancing lipid accumulation [Xu and Liao, 2004]. Insulin signaling during early differentiation involves insulin receptor tyrosine kinase activation, which triggers signaling events in the PI3K/Akt and Ras/MAPK pathways [Sakaue et al., 1998; Taniguchi et al., 2006a], both of which induce proliferation signaling during MCE [Qiu et al., 2001; Tang et al., 2003b; Nogueira et al., 2012]. Several lines of evidence also suggest that the inhibition of PI3K and extracellular-regulated kinase (ERK) impairs adipogenesis in 3T3-L1 preadipocytes [Tomiyama et al., 1995; Aubin et al., 2005].

Members of the botanical genus *Alnus* are well known for their traditional medicinal components which can be used as remedies for fever, hemorrhage, diarrhea, lymphatic disease, alcoholism, cancer, and diabetes [Lee, 1996; Kim et al., 2004; Hu et al., 2013]. Alder, a common name for *Alnus*, contains a variety of bioactive constituents, of which diarylheptanoids are the dominant group [Sati et al., 2011]. Recently, a study proposed a mechanism for the anti-adipogenic activity of diarylheptanoids from *Alnus hirsuta* f. *sibrica* using 3T3-L1 preadipocytes which involves the suppression of PPARγ and C/EBPα [Lee et al., 2013]. Hirsutenone (HST, Fig. 1) is an active form of diarylheptanoid, which can be isolated from *Alnus japonica* [Sati et al., 2011; Tung et al., 2010] and *A. hirsuta* [Sati et al., 2011]. Previous studies have shown that HST exhibits a wide range of biological activities, including anti-inflammatory, anti-tumor promoting and anti-atopic dermatitis effects [Kim et al., 2006; Jeong et al., 2010; Lee et al., 2010, 2012]. However, the anti-adipogenic properties of HST have not yet been investigated. We sought to investigate the effects of HST on adipocyte differentiation, the underlying mechanisms involved and its potential molecular target in 3T3-L1 preadipocytes.

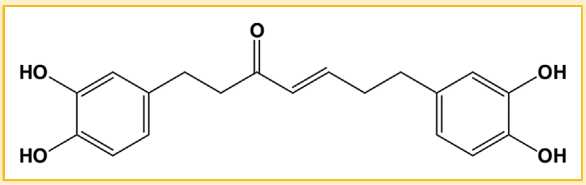

Fig. 1. The chemical structure of HST.

MATERIALS AND METHODS

CHEMICALS

DMEM and fetal bovine serum (FBS) were purchased from Welgene (Daegu, Republic of Korea). Bovine calf serum (BCS) was purchased from GIBCO (Grand Island, NY). Methylisobutylxantine (IBMX), dexamethasone, human insulin, and Oil Red O powder were purchased from Sigma (St. Louis, MO). 3-[4,5-Diethylthiazol-2-yl]-2,5-diphenyltetrazolium bromide (MTT) was purchased from USB Corporation (Cleveland, OH). Antibodies against PPARγ, total and p-ERK were purchased from Santa Cruz Biotechnology (Santa Cruz, CA). Antibodies against C/EBPα, FAS, total and p-Akt, RSK1/2/3, p-p90RSK, total and p-p70S6K were obtained from Cell Signaling Biotechnology (Beverly, MA).

SYNTHESIS OF HST

The compound HST was synthesized from curcumin according to literature published procedure with some modifications [Venkateswarlu et al., 2001]. In brief, hydrogenation of 1,6-diene double bonds of curcumin (1) with 10% pelladium on a carbon catalyst using parr hydrogenation apparatus afforded 1,7-bis(4-hydroxy-3-methoxyphenyl)heptane-3,5-dione (2) at 59% yield and compound 5-hydroxy-1,7-bis(4-hydroxy-3-methoxyphenyl)heptan-3-one (3) at 25% yield, respectively. Reduction of the carbonyl group of 1,7-bis(4-hydroxy-3-methoxyphenyl)heptane-3,5-dione (2) using sodium borohydride gave the compound 5-hydroxy-1,7-bis(4-hydroxy-3-methoxyphenyl)heptan-3-one (3) at 25% yield. Then, dehydration of 5-hydroxy-1,7-bis(4-hydroxy-3-methoxyphenyl)heptan-3-one (3) using p-toluenesulfonic acid as a catalyst gave (E)-1,7-bis(4-hydroxy-3-methoxyphenyl)hept-4-en-3-one (4) at 77% yield. Finally, demethylation of (E)-1,7-bis(4-hydroxy-3-methoxyphenyl)hept-4-en-3-one (4) using $AlCl_3$/pyridine afforded the desired compound HST, (E)-1,7-bis(3,4-dihydroxyphenyl)hept-4-en-3-one (5) at 20% yield (Fig. S1).

CELL CULTURE AND DIFFERENTIATION

3T3-L1 preadipocytes were purchased from the ATCC (Manassas, VA). The cells were maintained in DMEM supplemented with 10% BCS in an atmosphere of 5% CO_2 at 37°C until confluence. After 2 days post-confluence (designated as Day 0), cells were incubated in DMEM supplemented with 10% FBS and an adipogenic cocktail called MDI [dexamethasone (1 μM), IBMX (0.5 mM) and insulin (5 μg/ml)]. The media was changed to DMEM containing 10% FBS and insulin (5 μg/ml) on Day 2. On Day 4, cells were switched to DMEM containing 10% FBS. Preadipocytes were almost fully differentiated to adipocytes by Day 6.

CELL VIABILITY ASSAY

An MTT assay was performed to evaluate the effect of HST on cell viability. 3T3-L1 preadipocytes were seeded in 96-well plates at a density of 5.0×10^3 cells per well. After confluence, one group of cells were treated with MDI cocktail as a control while the rest were treated with MDI containing 20, 40, 80, or 100 μM of HST for 2 days. Subsequently, cells were incubated with MTT solution (0.5 mg/ml) for 1 h at 37°C. The violet formazan crystals were dissolved in DMSO and the absorbance was measured at 595 nm with a microplate reader (Beckman-Coulter, CA).

OIL RED O STAINING

3T3-L1 preadipocytes were seeded in 24-well plates at a density of 2.5×10^4 cells per well. After differentiation, cells were fixed with 4% formaldehyde for 1 h and then washed with phosphate buffered saline (PBS) three times. Next, cells were subjected to Oil Red O staining for 1 h to visualize accumulated lipid droplets in the cells. Stained cells were then washed with PBS three times, and intracellular lipid content was quantified by eluting Oil Red O stain with 100% isopropyl alcohol and measured at 515 nm with a microplate reader. Undifferentiated cells were served as the blank sample for this assay and isopropyl alcohol was used as background control to subtract the background signal from each of these the absorbance value.

WESTERN BLOT

3T3-L1 preadipocytes were seeded in 6-cm dishes at a density of 1.5×10^5 cells per well and treated as indicated. Cells were lysed and centrifuged for 10 min at 14,000 rpm at 4°C, and supernatants were collected. The supernatants were subjected to SDS–PAGE and transferred to a 0.2 μm Whatman nitrocellulose (NC) transfer membrane (GE Healthcare, Maidstone, UK). The membrane was blocked with 5% skim milk, followed by specific primary antibody incubation at 4°C overnight and HRP-conjugated secondary antibody. The protein bands were visualized using a chemiluminescence detection kit (Amersham Pharmacia Biotech; Piscataway, NJ).

FLUORESCENCE-ACTIVATED CELL SORTER (FACS) ANALYSIS

3T3-L1 preadipocytes were seeded in 6-cm dishes at a density of 1.0×10^5 cells per well. After 2 days post-confluence, cells were incubated in DMEM supplemented with 10% FBS and MDI cocktail in the presence or absence of 80 μM HST for 0, 20, 24, and 36 h. Cell pellets harvested at each time point were fixed in cold 70% (*v/v*) ethanol at 4°C overnight. Cells were then centrifuged for 3 min at 1,500 rpm and re-suspended in 600 μl of PBS containing 20 μg/ml of propidium iodide solution (PI) (Sigma; St. Louis, MO) and 0.2 mg/ml of RNase (Sigma; St. Louis, MO). Following incubation for 15 min at 37°C, fluorescence emitted from the cells was measured with a flow cytometer (Becton-Dickson, San Jose, CA). A total of 10,000 cells in each sample were analyzed.

TRYPAN BLUE ASSAY

3T3-L1 preadipocytes were seeded in 6-well plates at a density of 1.0×10^5 cells per well, and incubated in DMEM supplemented with 10% FBS and MDI cocktail in the presence or absence of 80 μM of HST for 24 and 48 h. Cells were then trypsinized and stained with 0.4% Trypan blue. The stained cells were loaded onto a hematocytometer and the viable cells were counted.

PI3K KINASE ASSAY

A kinase assay was performed as previously described [Seo et al., 2013]. Briefly, active PI3K protein (100 ng) was incubated with HST, at volumes of 20, 40, and 80 μM, or PI3K inhibitor LY294002 (20 μM), before 20 μl phosphatidylinositol (0.5 mg/ml; Avanti Polar Lipids, Alabaster, AL) was added. Reaction buffer (100 mM HEPES [pH 7.6], 50 mM $MgCl_2$ and 250 μM ATP) containing 10 μCi of [γ-^{32}P] ATP was then added and incubated for 10 min at 30°C. The reaction was stopped by adding 15 μl of 4 N HCl and 130 μl of a chloroform and methanol mixture (1:1). After vortexing, 30 μl of the lower chloroform phase was spotted onto 1% potassium oxalate-coated silica gel plates. The spotted chloroform phase was separated using thin-layer chromatography and radiolabeled spots were visualized by autoradiography.

ERK 1 KINASE ASSAY

The kinase assay reaction contained 5× reaction buffer [125 mM Tris/HCl pH 7.5 and 0.1 mM EGTA], active MAP kinase 1 [50 mM Tris/HCl pH 7.5, 0.1 mM EGTA, 0.1 mM sodium orthovanadate (Na_3VO_4), 0.1% 2-mercaptoethanol and 1 mg/ml BSA], together with magnesium acetate (MgAc)–ATP cocktail buffer [25 mM MgAc and 0.25 mM ATP]. Active ERK1 protein (10 ng) was incubated in the presence or absence of 20, 40, or 80 μM HST for 10 min at 30°C. Myelin Basic Protein (0.33 mM) substrate was added, followed by 10 μL of diluted [γ-^{32}P] ATP solution, before incubation at 30°C for 10 min with the reaction buffer and substrate peptide. 26 μL aliquots were transferred onto p81 filter paper followed by washing three times with 0.75% phosphoric acid and once with acetone. The incorporation of radioactivity was determined using a scintillation counter.

IN VITRO AND EX VIVO CO-IMMUNOPRECIPITATION ASSAY

Sepharose 4B freeze-dried powder (0.3 g; GE Healthcare, Buckinghamshire, UK) was activated in 1 mM HCl and suspended in HST (2 mg) coupled solution (0.1 M $NaHCO_3$ and 0.5 M NaCl). Following overnight rotation at 4°C, the mixture was transferred to 0.1 M Tris–HCl buffer (pH 8.0) and further rotated at 4°C overnight. The mixture was washed three times with 0.1 M acetate buffer (pH 4.0) and 0.1 M Tris–HCl + 0.5 M NaCl buffer (pH 8.0) respectively, and suspended in PBS. The immunoprecipitation assay was performed as previously described [Kang et al., 2008]. Briefly, active protein (ERK1 or PI3K) or cell lysate was incubated with Sepharose 4B alone or HST-Sepharose 4B beads in reaction buffer. After incubation at 4°C, the beads were washed in washing buffer and proteins bound to the beads were analyzed by immunoblotting.

ATP AND HST COMPETITION ASSAY

Active protein (0.2 μg; ERK1 or PI3K) was incubated with 100 μl of HST-Sepharose 4B or control Sepharose 4B beads in the presence or absence of 10 or 100 μM of ATP in the reaction buffer. The protein was immunoprecipitated and analyzed by immunoblotting following overnight incubation at 4°C.

STATISTICAL ANALYSIS

Data are expressed as mean ± SD values unless otherwise stated. Each group was compared by Student's t test where $P < 0.05$ was considered significant.

RESULTS

HST INHIBITS MDI-INDUCED ADIPOGENESIS IN 3T3-L1 PREADIPOCYTES

We first investigated the effect of HST on the differentiation of 3T3-L1 preadipocytes into mature adipocytes. 3T3-L1 preadipocytes were incubated in the presence or absence of HST (0, 20, 40, or 80 μM) during differentiation. As shown in the Oil Red O staining images, HST attenuated MDI-induced lipid accumulation in 3T3-L1 preadipocytes in a dose-dependent manner (Fig. 2A and B). In particular, HST at 40 and 80 μM significantly reduced MDI-induced adipogenesis in 3T3-L1 preadipocytes (Fig. 2B). Consistent with these results, we found that treatment of HST reduced the protein expression levels of PPARγ, C/EBPα, and FAS in a dose-dependent manner (Fig. 2C). In order to test whether this anti-adipogenic effect was a result of cytotoxicity, we examined the effects of HST on cell viability in preadipocytes. HST exerted no effect on cell viability of differentiating cells up to 100 μM concentration (Fig. 2D), but exhibited a 12% increase in lactate dehydrogenase release at 100 μM (data not shown). Collectively, these results show that non-toxic levels of HST (20, 40 and 80 μM) inhibit adipogenesis in 3T3-L1 preadipocytes.

HST PRIMARILY SUPPRESSES EARLY STAGE 3T3-L1 PREADIPOCYTE DIFFERENTIATION

To further evaluate the underlying molecular mechanisms of HST-dependent adipogenesis, we identified the adipogenic stages most affected by HST during differentiation of 3T3-L1 preadipocytes. Adipogenesis processes can be divided into three stages: the early

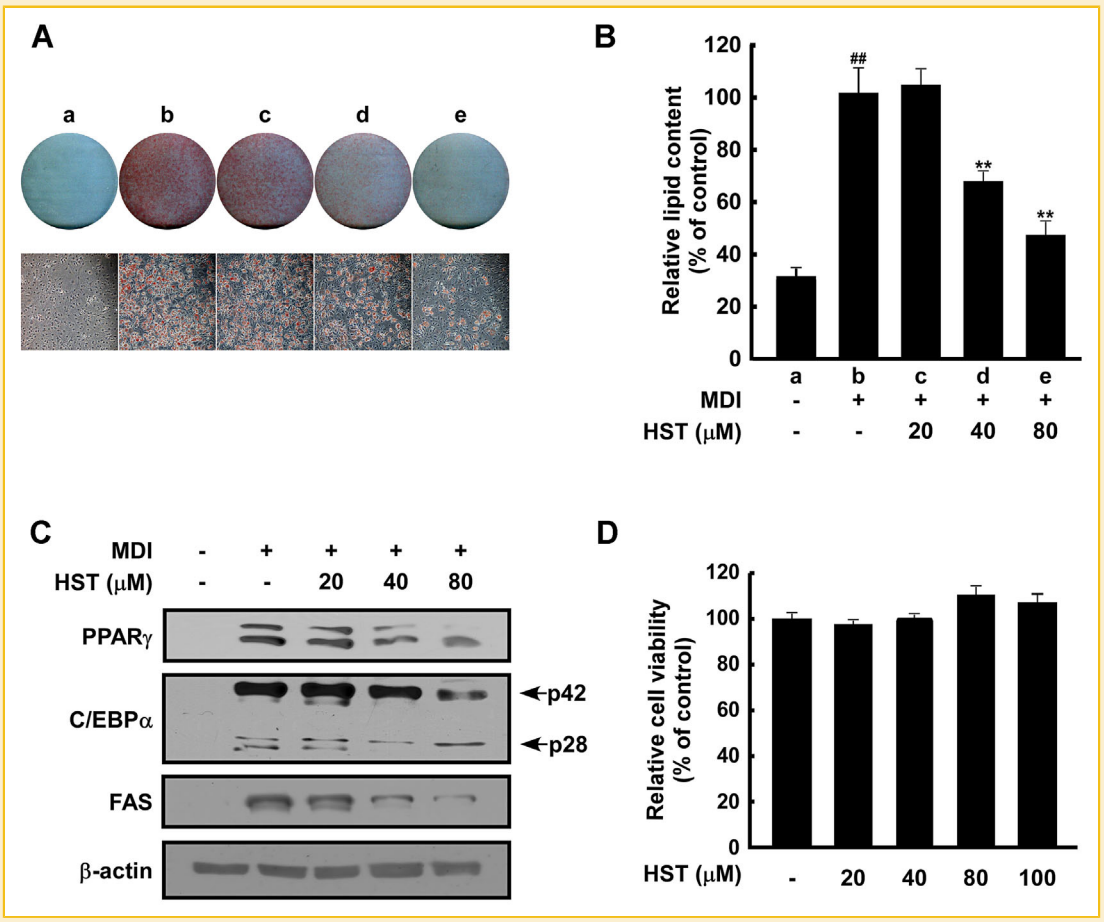

Fig. 2. HST inhibits adipogenesis in 3T3-L1 preadipocytes. A: Visualization of lipid accumulation by Oil Red O staining. Differentiating 3T3-L1 preadipocytes were treated with HST at different concentrations for 6 days. (a) Undifferentiated control, (b) differentiated control, (c) HST 20 μM, (d) HST 40 μM, and (e) HST 80 μM. B: The Oil Red O-stained lipid droplets in the differentiated cells were extracted with isopropanol for spectrometric quantification at 515 nm. Data are representative of three independent experiments that yielded similar results, which are presented as means ± SD. A significant difference is shown between the undifferentiated group and the MDI-treated group ($^{\#\#\#}P < 0.001$), as well as between the MDI-treated group and the group treated with MDI and HST ($^{**}P < 0.01$ and $^{***}P < 0.001$, respectively). C: HST suppressed MDI-induced PPARγ, C/EBPα expression and FAS expression levels after 6 days of differentiation as determined by Western blot analysis. D: 3T3-L1 preadipocytes were incubated with DMEM supplemented with 10% FBS, MDI and various concentrations of HST for 2 days. The cell viability was assessed by MTT assay. Cell viability was expressed as a percentage relative to control. Data are representative of three independent experiments that yielded similar results, which are presented as means ± SD.

stage (Day 0–2), the intermediate stage (Day 2–4) and the late stage (Day 4–6). Cells were differentiated in the presence or absence of HST (80 μM) for the indicated time periods as described in Figure 3A. Cells were subjected to Oil Red O staining of intracellular lipids after 6 days of differentiation (Fig. 3B, C). We observed that HST treatment for early stage differentiation (Day 0–2) caused a 43% reduction in lipid accumulation in the cells, whereas differentiating cells treated with HST during intermediate (Day 2–4) and late stages (Day 4–6) resulted in a 21% and 7% decrease in lipid content, respectively. In addition, the cells treated with HST at Day 2–6 showed an approximate 27% reduction in lipid accumulation when compared to the controls. Cells treated with HST at Days 0–4 and 0–6 showed a 60% reduction in lipid content. These results suggest that MDI-mediated lipid accumulation was decreased by HST treatment during Days 0–2, 0–4, and 0–6.

Additionally, HST treatment during the intermediate stage significantly reduced levels of lipid content in treated cells compared with controls, suggesting a possibility that HST has an additional role in modulating lipogenesis, which is known to occur in intermediate and late stages of adipogenesis. Collectively, these results show that

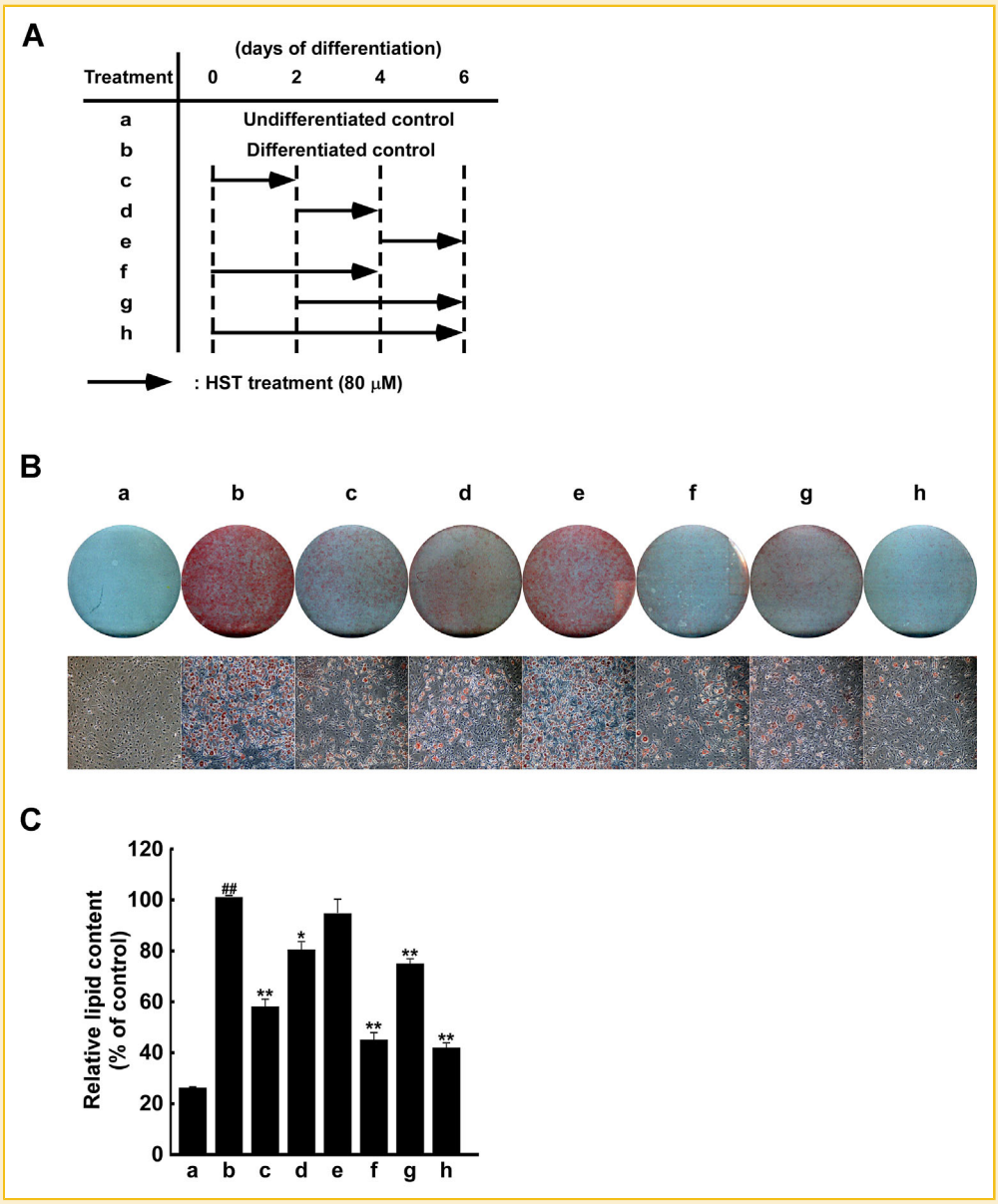

Fig. 3. Anti-adipogenic effects of HST are mainly contributable to inhibition of the early stage of adipogenesis. A: A schematic diagram of the treatment schedule of HST during 3T3-L1 differentiation. B: Visualization of lipid accumulation from Oil Red O-stained adipocytes. 80 μM HST was treated for the indicated duration during adipogenesis and cells were subjected to Oil Red O staining of intracellular lipid accumulation after 6 days of differentiation. C: Spectrometric quantification of stained adipocytes at 515 nm. Relative lipid content was expressed as % compared to the control (only the MDI-treated group). Data are representative of three independent experiments that yielded similar results, which are presented as means ± SD. A significant difference is shown between the undifferentiated group and MDI-treated group ($^{###}P < 0.001$), as well as between the MDI-treated group and the group treated with MDI and HST ($^{*}P < 0.05$ and $^{***}P < 0.001$, respectively).

HST exhibits inhibitory effects on adipogenesis, which primarily occurs in the early stage of adipogenesis.

HST DELAYS CELL CYCLE PROGRESSION DURING MCE IN 3T3-L1 PREADIPOCYTES

Since we observed that HST primarily exhibits its anti-adipogenic activities in MCE, we chose to further assess the effect of HST on the cell proliferation of 3T3-L1 preadipocytes. We quantified the total cell numbers at 24 and 48 h, after cell differentiation was induced by MDI. As expected, total cell numbers were increased in the MDI-treated group at 24 and 48 h, whereas HST treatment significantly suppressed the MDI-increased cell numbers (Fig. 4A). We next examined the effect of HST on cell cycle progression during the MCE process. Flow cytometry results (Fig. 4B) indicated that MDI induced cell cycle entry of differentiating preadipocytes into G2/M phase at 24 h, which is consistent with previous findings [Kwon et al., 2012a,b]. In the presence of 80 μM HST, a suppression of cell cycle entry to S and G2/M phases occurred at both 20 and 24 h. The majority of cells (65% of total cells) in the 80 μM HST-treated group were arrested in G1 phase when compared to the MDI-only treated group at 20 h (Fig. 4C). At 24 h, more cells were arrested in G1 phase (53% of total cells) when compared with the MDI-induced group which contained the majority of cells (56% of total cells) in G2/M phase. Further incubation of differentiating preadipocytes with HST to 36 h resulted in delayed cell cycle entry to S and G2/M phases compared with the MDI-only induced group. In addition, we also found that treatment of HST dose-dependently attenuates the expression of cyclin D1, and also reduced the protein expression of cyclin A1 (Fig. 4D). These results indicate that HST exhibits anti-adipogenesis effects by delaying cell cycle progression in the early stage of differentiation, and specifically, G1 phase arrest after 20 h of HST treatment.

HST REGULATES AKT- AND ERK-MEDIATED SIGNALING PATHWAYS BY SUPPRESSING PI3K AND ERK1 ACTIVITY

The downregulation of adipogenic transcription factors and induction of cell cycle arrest by HST led us to speculate on its potential

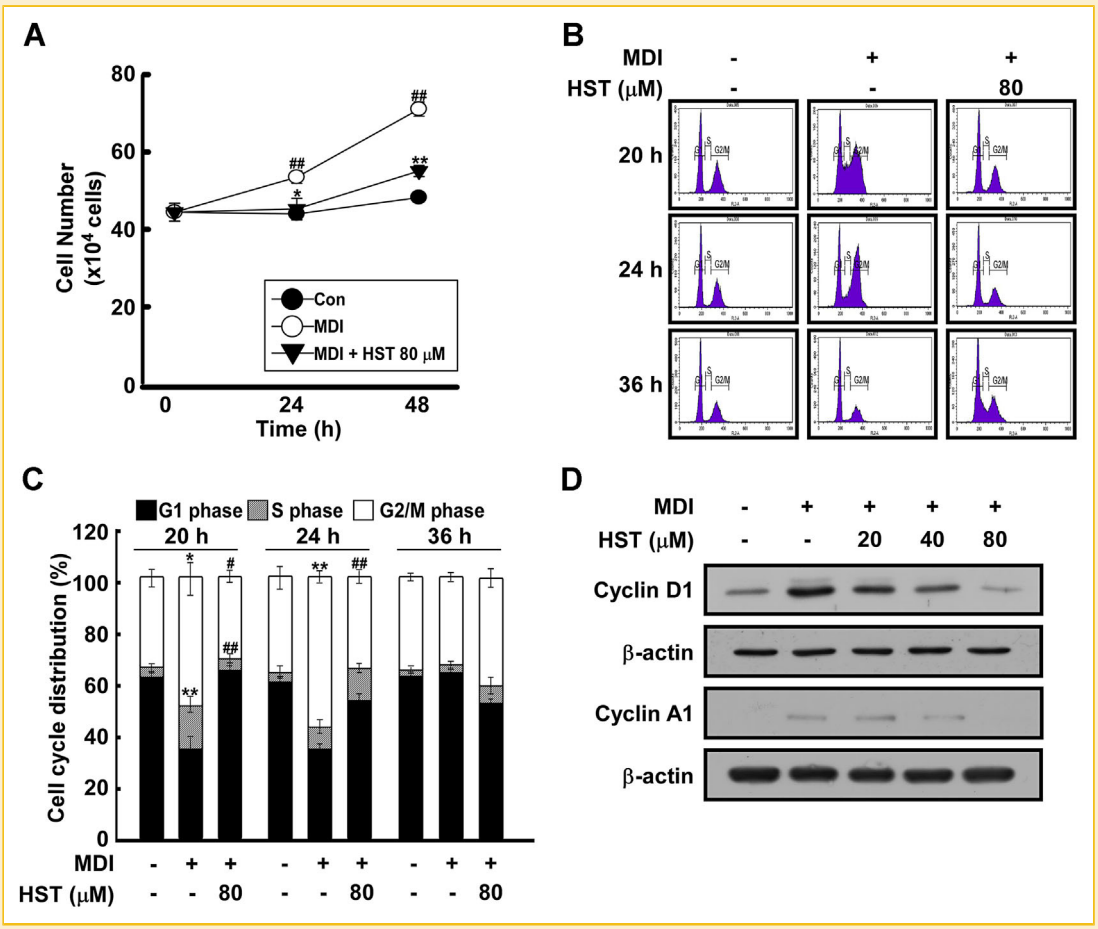

Fig. 4. HST suppresses cell proliferation and cell cycle progression during MCE of 3T3-L1 preadipocytes. A: The total cell numbers were evaluated by Trypan blue assays after 24 and 48 h of HST treatment. Data are representative of 3 independent experiments with similar results, which are presented as means ± S.D. B: Effects of HST on MDI-induced MCE in the early stage of adipogenesis. Cells were harvested at the indicated time after the initiation of differentiation with or without HST treatment and stained with PI solution for flow cytometer cell cycle analysis. The histogram results indicate cell cycle distribution in G1, S or G2/M phases. C: Quantitative data for cell cycle distribution at 20, 24, and 36 h of cell differentiation. D: HST suppressed MDI-induced Cyclin D1 and Cyclin A1 protein expression. Data are representative of three independent experiments with similar results, which are presented as means ± S.E. A significant difference is shown between the undifferentiated group and the MDI-treated group ($^{\#\#\#}P < 0.001$) as well as between the MDI-treated group and the group treated with MDI and HST ($^{*}P < 0.05$, $^{**}P < 0.01$ and $^{***}P < 0.001$, respectively).

effects on the PI3K/Akt and ERK signaling pathways, which are the two major signaling pathways mediating cell proliferation [Tang et al., 2003b]. HST treatment markedly reduced MDI-induced phosphorylation of Akt and its downstream effector protein p70S6K in a dose-dependent manner (Fig. 5A). Meanwhile, HST at 20, 40, and 80 μM did not affect the phosphorylation of ERK (Fig. 5B), but attenuated MDI-induced phosphorylation of p90RSK in a concentration-dependent manner.

To investigate whether the regulation of Akt- and ERK-mediated signaling pathways were occurring via the suppression of PI3K and ERK activity, kinase assays were performed. HST at 20, 40 and 80 μM exhibited a greater extent of inhibition in vitro on PI3K activity than 20 μM LY294002, a conventional PI3K inhibitor (Fig. 5C). According to previous studies, the ERK1 isoform, but not ERK2, is mainly involved in the regulation of adipocyte differentiation, adiposity and high-fat diet-induced obesity [Bost et al., 2005]. Thus, we measured the effect of HST on ERK1 activity in vitro (Fig. 5D). The results showed that HST at 20, 40, and 80 μM significantly suppressed ERK1 activity in a concentration-dependent manner. Taken together, our results suggest that HST induces cell cycle arrest by attenuating the activation of PI3K and ERK1, which leads to the downregulation of the Akt-mediated pathway and p90RSK phosphorylation.

HST DIRECTLY BINDS TO PI3K AND ERK1 IN AN ATP-NONCOMPETITIVE MANNER

To further investigate the mechanisms responsible for how HST inhibits PI3K and ERK1 activity, we evaluated the physical interaction between HST with PI3K and ERK1. We performed in vitro and ex vivo immunoprecipitation assays for PI3K and ERK1 protein using HST-conjugated Sepharose 4B beads. The results showed that PI3K precipitated with HST-conjugated Sepharose 4B beads both in vitro and ex vivo, indicating a physical binding interaction between PI3K and HST (Fig. 6A, B). Similarly, ERK1 was also shown to bind to HST-Sepharose 4B beads both in vitro and ex vivo (Fig. 6C, D), and binding of HST to both PI3K and ERK1 occurred in an ATP-noncompetitive manner (Fig. 6E, F). These results suggest that HST and ATP interact with PI3K and ERK1 at different binding sites.

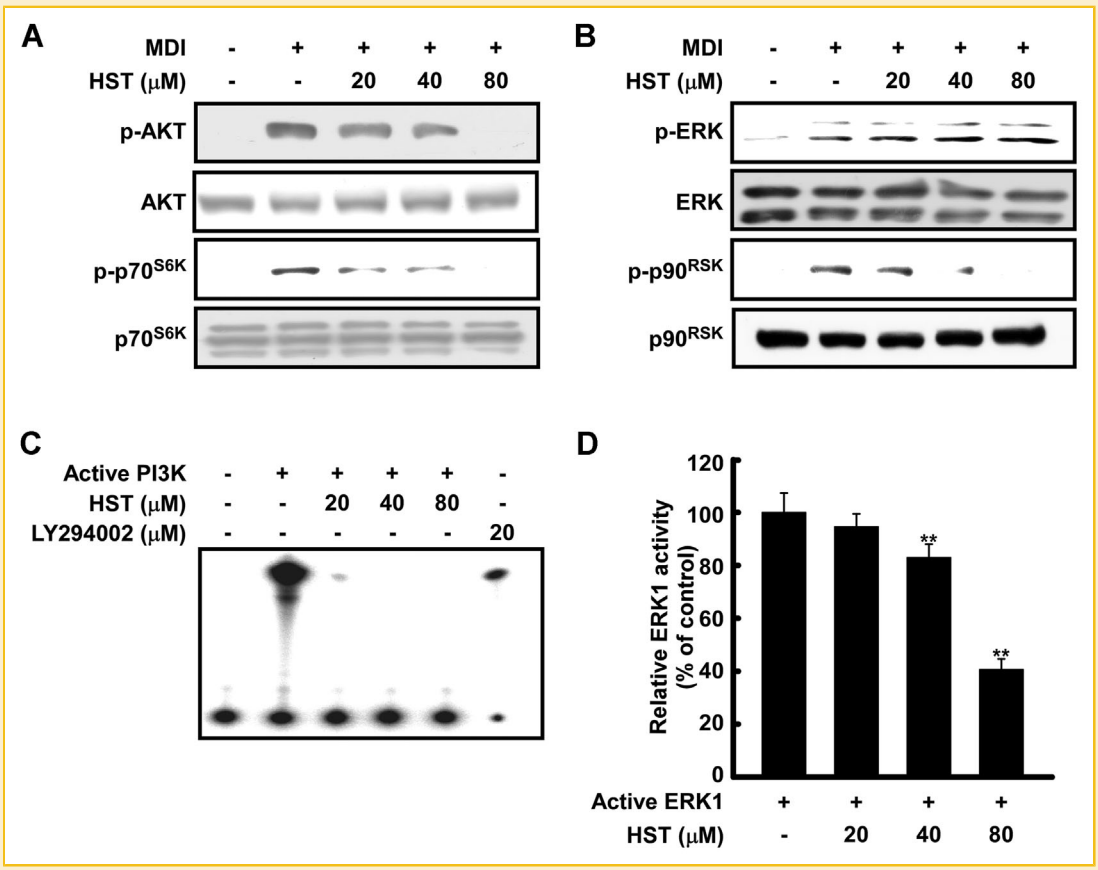

Fig. 5. HST inhibits PI3K and ERK1 activity in the early phase of adipogenesis. A: Levels of phosphorylated Akt (Ser473) and p-p70S6K in differentiating cells treated with 20, 40 and 80 μM HST for 1 h were measured by Western blot analysis. B: Phosphorylated ERK and p90RSK in differentiating cells treated with 20, 40, and 80 μM HST for 15 min were analyzed by Western blot analysis. All data are representative of three independent experiments that yielded similar results. C: HST suppresses in vitro PI3K activity. The 32P-labeled phosphatidylinositol-3-phosphate product was resolved through thin layer chromatography and visualized by autoradiography. D: HST inhibits in vitro ERK1 activity. Kinase activity is expressed as percentage of relative ERK1 kinase activity. All data are representative of three independent experiments that yielded similar results, which are presented as means ± SD. A significant difference is been shown between the undifferentiated group and the MDI-treated group ($^{\#\#\#}P < 0.001$), as well as between the MDI-treated group and the group treated with MDI and HST ($^{*}P < 0.05$, $^{**}P < 0.01$, and $^{***}P < 0.001$, respectively.

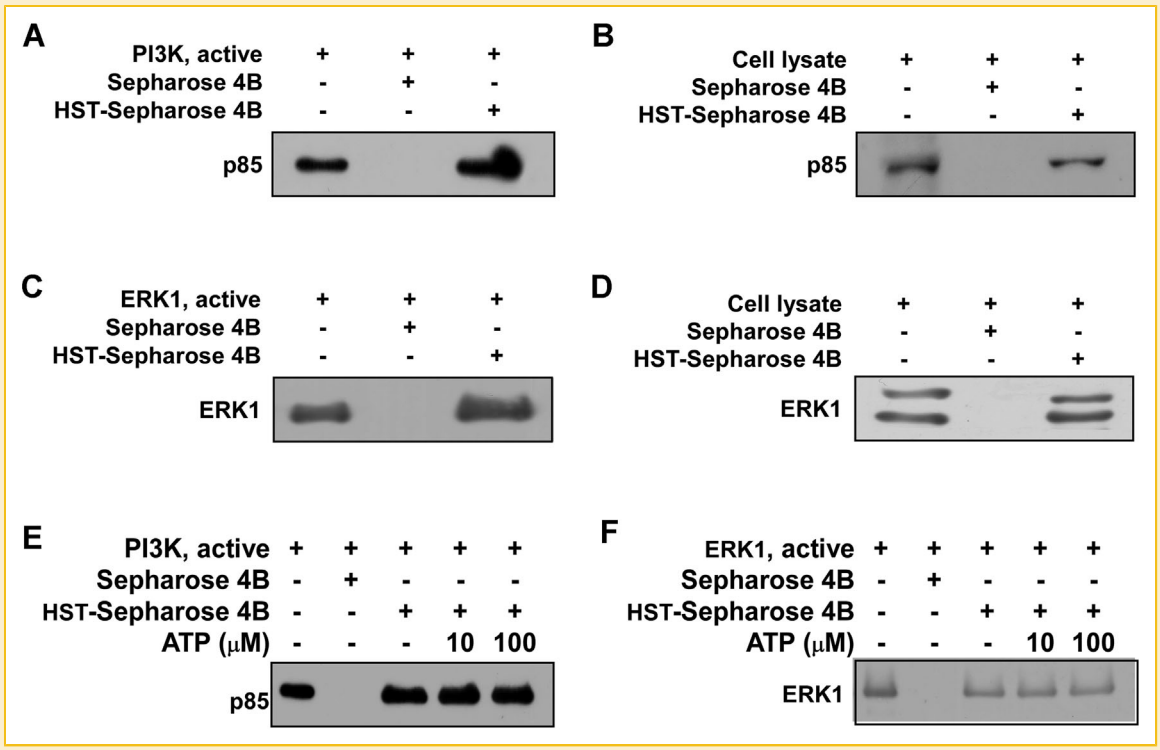

Fig. 6. HST directly binds to PI3K and ERK1 in an ATP-noncompetitive manner. A, B: *In vitro* and ex vivo binding of HST with PI3K. Lane 1, active PI3K (100 ng); lane 2, negative control; lane 3, active PI3K bound to HST-Sepharose 4B beads. C, D: In vitro and ex vivo binding of HST with ERK. Lane 1, active ERK1 (10 ng); lane 2, negative control; lane 3: active ERK1 bound to HST-Sepharose 4B. E: HST binds with PI3K in an ATP-noncompetitive manner. F: HST binds with ERK in an ATP-noncompetitive manner. Data are representative of three independent experiments that yielded similar results.

DISCUSSION

In this study, non-toxic levels of HST were found to exert anti-adipogenic effects, which were largely limited to the early stage of adipogenesis. The HST-mediated suppression of cell proliferation is associated with delayed cell cycle progression and an interaction with PI3K and ERK1 during MDI-induced adipogenesis of 3T3-L1 preadipocytes. However, whether MCE is an imperative early stage in the initiation of adipocyte differentiation remains controversial [Danesch et al., 1992; Rosen et al., 2000; Qiu et al., 2001; Tang et al., 2003b]. Several studies have demonstrated that modulation of MCE can inhibit adipogenesis in 3T3-L1 cells [Li et al., 2007; Kim et al., 2011; Choi et al., 2012; Kwon et al., 2012a,b]. For instance, cocoa polyphenol extracts have been demonstrated to suppress MCE during adipogenesis via inactivation of IR, which has also been confirmed in a diet-induced obese animal model [Min et al., 2013].

In addition to its inhibitory effects on the early stage of adipogenesis, we also observed that HST reduced lipid accumulation during the intermediate stage including Days 2–4, although it was not as effective as that occurring in the MCE stage. Likewise, we found that HST is able to reduce the protein expression levels of FAS as well as PPARγ and C/EBPα during adipogenesis of 3T3-L1 preadipocytes. FAS is a lipogenic enzyme that is involved in the synthesis and storage of triglycerides [Claycombe et al., 1998]. Previous studies have reported that adipocyte differentiation is blocked after being treatment with the FAS inhibitor C75 [Liu et al., 2004]. This finding indicates that the inhibitory effects of HST in adipogenesis may not be limited to MCE, but might also extend to anti-adipogenic effects via regulation of lipogenesis.

We found no evidence for an inhibitory effect of tyrosine phosphorylation of the insulin receptor in HST-treated cells (data not shown). Nevertheless, HST downregulated Akt signaling (Fig. 5A) and PI3K in vitro (Fig. 6A). This is in agreement with findings from previous studies showing that disruption of Akt and PI3K can inhibit the differentiation of preadipocytes into adipocytes [Xia and Serrero, 1999; Xu and Liao, 2004; Aubin et al., 2005; Baudry et al., 2006; Zhang et al., 2009]. In particular, the anti-adipogenic activity of phytochemicals that inhibit PI3K activation have been widely investigated. HST is a highly potent inhibitor of PI3K kinase activity in vitro [Farrand et al., 2014].

Insulin is known to induce lipogenesis and glucose uptake in mature adipocytes. Insulin-induced Akt and ERK signaling pathways are also required for cell cycle progression during adipogenesis, as demonstrated in insulin receptor-deficient mice [Bluher et al., 2002, 2004]. Although the insulin signaling pathway is involved in the early phase of cell differentiation via the modulation of cell cycle progression and promotion of adipogenesis (thereby potentially increasing hyperplasia), suppressing this pathway might lead to insulin resistance [Okada et al., 1994; Shepherd et al., 1995; Carvalho et al., 2000]. Besides adipose tissue, other insulin sensitive tissues and

organs, such as the liver, muscles and hypothalamus, are also involved in the inter-tissue communication responsible for the regulation of insulin action. Therefore, tissue-specific effects of HST on the PI3K/Akt pathway and their impact on insulin sensitivity should be further explored. In a previous study, genetic disruption of the p85α regulatory subunit of PI3K increased hepatic and peripheral insulin sensitivity, although PI3K enzymatic activity was diminished in the liver [Taniguchi et al., 2006b]. In addition, it has been revealed that a herb formula extract derived from *A. hirsuta* bark has strong potential anti-diabetic effects [Hu et al., 2013]. Since HST is one of the main bioactive compounds in *A. hirsuta*, there is a high possibility that HST could contribute to the attenuation of adipogenesis without triggering insulin resistance. However, further studies are necessary to examine the effect of HST on insulin sensitivity in vivo.

In conclusion, a new role for HST in adipogenesis has been discovered, which primarily involves targeting of the early phase of differentiation (MCE) and a subsequent phosphorylation cascade of the insulin-signaling pathway resulting in suppression of PPARγ and C/EBPα. Taken together, these findings provide important insights into the mechanisms underlying the anti-obesity activities of HST. Further studies utilizing in vivo system are still required to determine the efficacy of HST in physiological condition. This may provide an important foundation for the development of therapeutics to prevent obesity and obesity-related metabolic diseases.

ACKNOWLEDGEMENTS

This work was supported by the Leap Research Program (2010-0029233) and the National Research Foundation (2012M3A9C4048818) funded by the Ministry of Science, ICT and Future Planning, Republic of Korea.

REFERENCES

Anthony NM, Gaidhu MP, Ceddia RB. 2009. Regulation of visceral and subcutaneous adipocyte lipolysis by acute AICAR-induced AMPK activation. Obesity (Silver Spring) 17:1312–1317.

Aubin D, Gagnon A, Sorisky A. 2005. Phosphoinositide 3-kinase is required for human adipocyte differentiation in culture. Int J Obes (Lond) 29:1006–1009.

Baudry A, Yang ZZ, Hemmings BA. 2006. PKBalpha is required for adipose differentiation of mouse embryonic fibroblasts. J Cell Sci 119:889–897.

Bluher M, Michael MD, Peroni OD, Ueki K, Carter N, Kahn BB, Kahn CR. 2002. Adipose tissue selective insulin receptor knockout protects against obesity and obesity-related glucose intolerance. Dev Cell 3:25–38.

Bluher M, Patti ME, Gesta S, Kahn BB, Kahn CR. 2004. Intrinsic heterogeneity in adipose tissue of fat-specific insulin receptor knock-out mice is associated with differences in patterns of gene expression. J Biol Chem 279:31891–31901.

Bost F, Aouadi M, Caron L, Even P, Belmonte N, Prot M, Dani C, Hofman P, Pagès G, Pouysségur J. 2005. The extracellular signal–regulated kinase isoform ERK1 is specifically required for in vitro and in vivo adipogenesis. Diabetes 54:402–411.

Carvalho E, Rondinone C, Smith U. 2000. Insulin resistance in fat cells from obese Zucker rats – evidence for an impaired activation and translocation of protein kinase B and glucose transporter 4. Mol Cell Biochem 206:7–16.

Choi KM, Lee YS, Sin DM, Lee S, Lee MK, Lee YM, Hong JT, Yun YP, Yoo HS. 2012. Sulforaphane inhibits mitotic clonal expansion during adipogenesis through cell cycle arrest. Obesity (Silver Spring) 20:1365–1371.

Claycombe KJ, Jones BH, Standridge MK, Guo Y, Chun JT, Taylor JW, Moustaid-Moussa N. 1998. Insulin increases fatty acid synthase gene transcription in human adipocytes. Am J Physiol 274:R1253–1259.

Cristancho AG, Lazar MA. 2011. Forming functional fat: A growing understanding of adipocyte differentiation. Nat Rev Mol Cell Biol 12: 722–734.

Danesch U, Hoeck W, Ringold GM. 1992. Cloning and transcriptional regulation of a novel adipocyte-specific gene, FSP27. CAAT-enhancer-binding protein (C/EBP) and C/EBP-like proteins interact with sequences required for differentiation-dependent expression. J Biol Chem 267:7185–7193.

de Ferranti S, Mozaffarian D. 2008. The perfect storm: obesity, adipocyte dysfunction, and metabolic consequences. Clin Chem 54:945–955.

Farrand L, Kim JY, Byun S, Im-aram A, Lee J, Suh JY, Lee KW, Lee HJ, Tsang BK. 2014. The diarylheptanoid hirsutenone sensitizes chemoresistant ovarian cancer cells to cisplatin via modulation of apoptosis-inducing factor and X-linked inhibitor of apoptosis. J Biol Chem 289:1723–1731.

Hu W, Yeo JH, Jiang Y, Heo SI, Wang MH. 2013. The antidiabetic effects of an herbal formula composed of *Alnus hirsuta*, Rosa davurica, Acanthopanax senticosus and Panax schinseng in the streptozotocin-induced diabetic rats. Nutr Res Pract 7:103–108.

Jeong MS, Choi SE, Kim JY, Kim JS, Kim EJ, Park KH, Lee do I, Joo SS, Lee CS, Bang H, Lee MK, Choi YW, Li KS, Moon NJ, Lee MW, Seo SJ. 2010. Atopic dermatitis-like skin lesions reduced by topical application and intraperitoneal injection of Hirsutenone in NC/Nga mice. Clin Dev Immunol 2010:618517.

Kang NJ, Lee KW, Lee DE, Rogozin EA, Bode AM, Lee HJ, Dong Z. 2008. Cocoa procyanidins suppress transformation by inhibiting mitogen-activated protein kinase kinase. J Biol Chem 283:20664–73.

Kim CY, Le TT, Chen C, Cheng JX, Kim KH. 2011. Curcumin inhibits adipocyte differentiation through modulation of mitotic clonal expansion. J Nutr Biochem 22:910–920.

Kim JH, Lee KW, Lee MW, Lee HJ, Kim SH, Surh YJ. 2006. Hirsutenone inhibits phorbol ester-induced upregulation of COX-2 and MMP-9 in cultured human mammary epithelial cells: NF-kappaB as a potential molecular target. FEBS Lett 580:385–392.

Kim ST, Kim JD, Ahn SH, Ahn GS, Lee YI, Jeong YS. 2004. Hepatoprotective and antioxidant effects of Alnus japonica extracts on acetaminophen-induced hepatotoxicity in rats. Phytother Res 18:971–975.

Kwon JY, Seo SG, Heo YS, Yue S, Cheng JX, Lee KW, Kim KH. 2012a. Piceatannol, natural polyphenolic stilbene, inhibits adipogenesis via modulation of mitotic clonal expansion and insulin receptor-dependent insulin signaling in early phase of differentiation. J Biol Chem 287:11566–11578.

Kwon JY, Seo SG, Yue S, Cheng JX, Lee KW, Kim KH. 2012b. An inhibitory effect of resveratrol in the mitotic clonal expansion and insulin signaling pathway in the early phase of adipogenesis. Nutr Res 32:607–616.

Lai CS, Tsai ML, Badmaev V, Jimenez M, Ho CT, Pan MH. 2012. Xanthigen suppresses preadipocyte differentiation and adipogenesis through down-regulation of PPARgamma and C/EBPs and modulation of SIRT-1, AMPK, and FoxO pathways. J Agric Food Chem 60:1094–1101.

Lee SJ. 1996. Korea folk medicine. Seoul: Seoul National University Publishing Center Press. p40.

Lee CS, Jang ER, Kim YJ, Lee MS, Seo SJ, Lee MW. 2010. Hirsutenone inhibits lipopolysaccharide-activated NF-kappaB-induced inflammatory mediator production by suppressing Toll-like receptor 4 and ERK activation. Int. Immunopharmacol 10:520–525.

Lee CS, Jang ER, Kim YJ, Myung SC, Kim W, Lee MW. 2012. Diarylheptanoid hirsutenone enhances apoptotic effect of TRAIL on epithelial ovarian carcinoma cell lines via activation of death receptor and mitochondrial pathway. Invest New Drugs 30:548–557.

Lee M, Song JY, Chin YW, Sung SH. 2013. Anti-adipogenic diarylheptanoids from *Alnus hirsuta* f. sibirica on 3T3-L1 cells. Bioorg Med Chem Lett 23: 2069–2073.

Li X, Kim JW, Gronborg M, Urlaub H, Lane MD, Tang QQ. 2007. Role of cdk2 in the sequential phosphorylation/activation of C/EBPbeta during adipocyte differentiation. Proc. Natl. Acad Sci U S A 104:11597–11602.

Liu LH, Wang XK, Hu YD, Kang JL, Wang LL, Li S. 2004. Effects of a fatty acid synthase inhibitor on adipocyte differentiation of mouse 3T3-L1 cells. Acta Pharmacol Sin 25:1052–1057.

Min SY, Yang H, Seo SG, Shin SH, Chung MY, Kim J, Lee SJ, Lee HJ, Lee KW. 2013. Cocoa polyphenols suppress adipogenesis in vitro and obesity in vivo by targeting insulin receptor. Int J Obes (Lond) 37:584–592.

Mishra S, Sachan A, Sachan SG. 2013. Production of natural value-added compounds: an insight into the eugenol biotransformation pathway. J Ind Microbiol Biotechnol 40:545–550.

Nogueira V, Sundararajan D, Kwan JM, Peng XD, Sarvepalli N, Sonenberg N, Hay N. 2012. Akt-dependent Skp2 mRNA translation is required for exiting contact inhibition, oncogenesis, and adipogenesis. EMBO J 31:1134–1146.

Okada T, Kawano Y, Sakakibara T, Hazeki O, Ui M. 1994. Essential role of phosphatidylinositol 3-kinase in insulin-induced glucose transport and antilipolysis in rat adipocytes. Studies with a selective inhibitor wortmannin. J Biol Chem 269:3568–3573.

Qiu Z, Wei Y, Chen N, Jiang M, Wu J, Liao K. 2001. DNA synthesis and mitotic clonal expansion is not a required step for 3T3-L1 preadipocyte differentiation into adipocytes. J Biol Chem 276:11988–11995.

Rosen ED, Walkey CJ, Puigserver P, Spiegelman BM. 2000. Transcriptional regulation of adipogenesis. Genes Dev 14:1293–1307.

Sakaue H, Ogawa W, Matsumoto M, Kuroda S, Takata M, Sugimoto T, Spiegelman BM, Kasuga M. 1998. Posttranscriptional control of adipocyte differentiation through activation of phosphoinositide 3-kinase. J Biol Chem 273:28945–28952.

Sati SC, Sati N, Sati OP. 2011. Bioactive constituents and medicinal importance of genus Alnus. Pharmacogn Rev 5:174–183.

Seo SG, Yang H, Shin SH, Min SY, Kim YA, Yu JG, Lee DE, Chung MY, Heo YS, Kwon JY, Yue SH, Kim KH, Cheng JX, Lee KW, Lee HJ. 2013. A metabolite of daidzein, 6,7,4′-trihydroxyisoflavone, suppresses adipogenesis in 3T3-L1 preadipocytes via ATP-competitive inhibition of PI3K. Mol Nutr Food Res 57(8):1446–1455.

Shepherd PR, Nave BT, Siddle K. 1995. Insulin stimulation of glycogen-synthesis and glycogen-synthase activity is blocked by wortmannin and rapamycin in 3t3-L1 adipocytes – evidence for the involvement of Phosphoinositide 3-kinase and P70 ribosomal protein-S6 kinase. Biochem J 305:25–28.

Sun L, Goff LA, Trapnell C, Alexander R, Lo KA, Hacisuleyman E, Sauvageau M, Tazon-Vega B, Kelley DR, Hendrickson DG, Yuan B, Kellis M, Lodish HF, Rinn JL. 2013. Long noncoding RNAs regulate adipogenesis. Proc Natl Acad Sci U S A 110:3387–3392.

Tang QQ, Otto TC, Lane MD. 2003a. CCAAT/enhancer-binding protein beta is required for mitotic clonal expansion during adipogenesis. Proc Natl Acad Sci U S A 100:850–855.

Tang QQ, Otto TC, Lane MD. 2003b. Mitotic clonal expansion: a synchronous process required for adipogenesis. Proc Natl Acad Sci U S A 100:44–49.

Taniguchi CM, Emanuelli B, Kahn CR. 2006a. Critical nodes in signalling pathways: insights into insulin action. Nat Rev Mol Cell Biol 7:85–96.

Taniguchi CM, Tran TT, Kondo T, Luo J, Ueki K, Cantley LC, Kahn CR. 2006b. Phosphoinositide 3-kinase regulatory subunit p85alpha suppresses insulin action via positive regulation of PTEN. Proc Natl Acad Sci U S A 103:12093–12097.

Tomiyama K, Nakata H, Sasa H, Arimura S, Nishio E, Watanabe Y. 1995. Wortmannin, a specific phosphatidylinositol 3-kinase inhibitor, inhibits adipocytic differentiation of 3T3-L1 cells. Biochem Biophys Res Commun 212:263–269.

Tung NH, Kim SK, Ra JC, Zhao YZ, Sohn DH, Kim YH. 2010. Antioxidative and hepatoprotective diarylheptanoids from the bark of *Alnus japonica*. Planta Med 76:626–670.

Venkateswarlu S, Ramachandra M, Rambabu M, Subbaraju GV. 2001. Synthesis of Gingerenone A and Hirsutenone. Indian J Chem Sect B 40:495–497.

Witczak C, Sharoff C, Goodyear L. 2008. AMP-activated protein kinase in skeletal muscle: from structure and localization to its role as a master regulator of cellular metabolism. Cell Mol Life Sci 65:3737–3755.

Xia X, Serrero G. 1999. Inhibition of adipose differentiation by phosphatidylinositol 3-kinase inhibitors. J. Cell Physiol 178:9–16.

Xu J, Liao K. 2004. Protein kinase B/AKT 1 plays a pivotal role in insulin-like growth factor-1 receptor signaling induced 3T3-L1 adipocyte differentiation. J Biol Chem 279:35914–35922.

Zhang HH, Huang J, Duvel K, Boback B, Wu S, Squillace RM, Wu CL, Manning BD. 2009. Insulin stimulates adipogenesis through the Akt-TSC2-mTORC1 pathway. PLoS ONE 4:e6189.

Zhang JW, Tang QQ, Vinson C, Lane MD. 2004. Dominant-negative C/EBP disrupts mitotic clonal expansion and differentiation of 3T3-L1 preadipocytes. Proc Natl Acad Sci U S A 101:43–47.

SUPPORTING INFORMATION

Additional Supporting Information may be found in the online version of this article at the publisher's web-site.